Plasma properties of helium gas tungsten arc with metal vapour

S. Tashiro*[1], M. Tanaka[1], K. Nakata[1], T. Iwao[2], F. Koshiishi[3], K. Suzuki[3] and K. Yamazaki[3]

The energy source characteristics of gas tungsten arc (GTA) strongly depend on the physical property of arc plasma. In welding processes, it has been experimentally confirmed that metal vapour evaporated from a high temperature weld pool drastically changes the property of arc plasma and decreases its temperature. However, the effect of metal vapour on the characteristics of heat flux into a base metal is still not clear owing to the difficulty in experimental studies of arc plasma. In the present paper, the energy source property of helium GTA mixed with metal vapour was numerically analysed. It was found that the intense radiation generated from dense metal vapour decreases heat flux into a base metal and contracts the current density distribution especially near the arc axis.

Keywords: Numerical simulation, Gas tungsten arc, Helium, Metal vapour, Heat input, Radiation

Introduction

In an arc welding process such as gas metal arc (GMA), it has been experimentally confirmed that a large quantity of metal vapour evaporated from a weld pool and high temperature metal droplets at the tip of a welding wire drastically changes the physical property such as electrical conductivity of arc plasma. The mixture of metal vapour decreases the temperature of arc plasma resulting in the reduction in heat flux into a base metal. Therefore it is important to understand the effect of the mixture of metal vapour on the arc welding process to improve the efficiency of welding.

A number of experimental investigations of the temperature distribution of arc plasma mixed with metal vapour in gas tungsten arc (GTA) have been conducted. For example, the plasma spectroscopic observation of argon (Ar) GTA[1,2] and nitrogen (N_2) GTA[3] revealed that the mixture of metal vapour increases the electrical conductivity of arc plasma and that the temperature consequently decreases by $\sim$2000 K in the vicinity of the anode (the weld pool) in comparison with the cases of pure Ar and pure N_2 GTA. Recently, helium (He) GTA using SUS304 as a base metal was also investigated and it was found that the mixture ratio of metal vapour reaches a level of 5% and the temperature decreases by $\sim$6000 K near the fringe of the arc column.[4–6] On the other hand, it was also reported that the mixture hardly affects the temperature distribution in high arc current welding since metal vapour is swept away by strong cathode jets.[7] The computation analysis of Ar GTA with the mixture of copper[8] and iron[9] vapour was conducted using a magnetic–hydrodynamic modelling and it was found that the temperature decreases by 2000 K near the anode in comparison with the case of pure Ar GTA.

In contrast to the above phenomena, it is well known that a large quantity of metal vapour is generated from not only a weld pool but also metal droplets at the tip of a wire in the case of GMA. Figure 1 shows the photographs of He GTA[4–6] and He GMA. It is obvious that the most part of the arc column in the He GTA is purple inherent in pure He plasma because the mixture of metal vapour is limited only on the anode (molten weld pool). On the contrary, metal vapour is mixed in the entire arc column in GMA and the arc column becomes blue inherent in metal vapour plasma. It is thus expected that the influence of the metal vapour mixture on the plasma property is more significant in GMA than that in GTA. In GMA, not only the plasma phenomenon but also the droplet formation at the tip of a wire have to be considered and thus, a highly sophisticated modelling is required. Recently several simulation models for GMA have been developed.[10–13] However, the effect of the metal vapour mixture has not been considered yet.

The present study avoided analysing the complex phenomena such as formation, breakaway and transfer of droplets and assumed that a large quantity of metal vapour is mixed uniformly in the entire arc plasma as observed in GMA. The plasma property of He GTA is numerically analysed as a virtual experiment and the results of the evaluation of the characteristics of heat flux into the anode are reported. A water cooled copper anode was employed as a base metal since it was confirmed to be suitable in evaluating the heat flux characteristics.[14] In addition, only iron vapour was assumed as the mixture component for simplicity.

[1]Joining and Welding Research Institute, Osaka University, 11-1 Mihogaoka, Ibaraki, Osaka, 576-0047, Japan
[2]Musashi Institute of Technology, 1-28-1, Tamadutsumi, Setagaya, Tokyo, 158-8577, Japan
[3]Kobe Steel, Ltd, 100-1, Miyamae, Fujisawa, Kanagawa, 251-8551, Japan

*Corresponding author, email tashiro@jwri.osaka-u.ac.jp

Published by Maney on behalf of the Institute
Received 24 August 2006; accepted
DOI 10.1179/174329307X164391

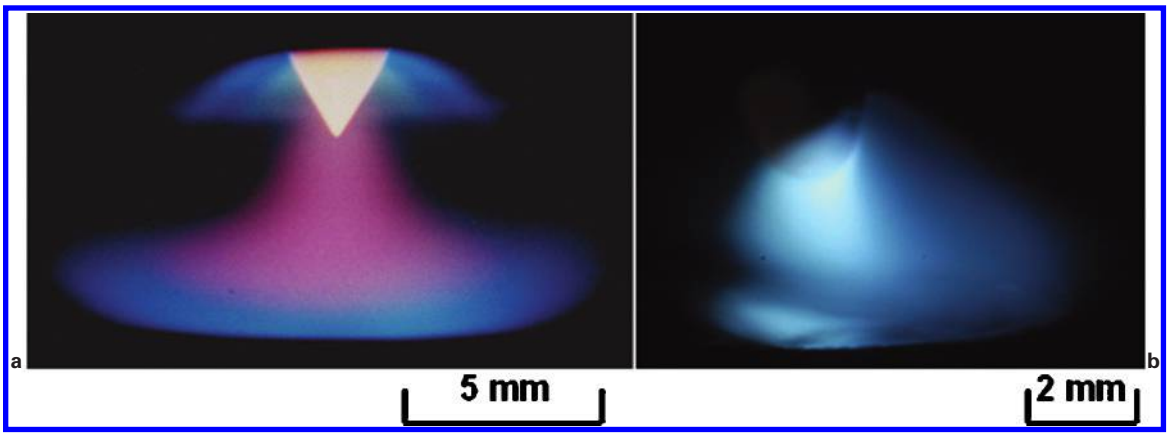

1 Photographs of *a* GTA and *b* GMA welding with pure He at arc current of 150 A

Simulation model

Figure 2 shows the calculation region representing GTA which consists of a tungsten cathode with a diameter of 3·2 mm and a tip angle of 60°, arc plasma and a water cooled copper anode. It is described in a frame of cylindrical coordinate with axial symmetry around the arc axis. The lengths of AC and AF are 45 and 25 mm respectively. The electrode gap is set to be 5 mm. The constant arc current of 150 A is given inside the cathode. The shielding gas is introduced from the upper boundary at the flowrate of 10 L min^{-1}. As explained in the introduction, it is obvious that a large amount of metal vapour is mixed in the arc plasma of GMA compared with the GTA. In the present study, the cases of the mixture ratios of 5, 10, 20 and 30% which are higher than those examined in the previous study[6] are investigated in addition to pure He GTA. The laminar flow is assumed, and the arc plasma is considered to be in the local thermodynamic equilibrium (LTE). The other numerical modelling methods are given in detail in previous papers[15,16] which were extended from the Lowke's work.[17] The differential equations (1)–(6) are solved iteratively by the SIMPLEC numerical procedure.[18]

Mass continuity equation is

$$\frac{1}{r}\frac{\partial}{\partial r}(r\rho v_r)+\frac{\partial}{\partial z}(\rho v_z)=0 \tag{1}$$

Radial momentum conservation equation is

$$\frac{1}{r}\frac{\partial}{\partial r}(r\rho v_r^2)+\frac{\partial}{\partial z}(\rho v_r v_z)=-\frac{\partial P}{\partial r}-j_z B_\theta+\frac{1}{r}\frac{\partial}{\partial r}\left(2r\eta\frac{\partial v_r}{\partial r}\right)+\frac{\partial}{\partial z}\left(\eta\frac{\partial v_r}{\partial z}+\eta\frac{\partial v_z}{\partial r}\right)-2\eta\frac{v_r}{r^2} \tag{2}$$

Axial momentum conservation equation is

$$\frac{1}{r}\frac{\partial}{\partial r}(r\rho v_r v_z)+\frac{\partial}{\partial z}(\rho v_z^2)=-\frac{\partial P}{\partial z}+j_r B_\theta+\frac{\partial}{\partial z}\left(2\eta\frac{\partial v_z}{\partial z}\right)+\frac{1}{r}\frac{\partial}{\partial r}\left(r\eta\frac{\partial v_r}{\partial z}+r\eta\frac{\partial v_z}{\partial r}\right) \tag{3}$$

Energy conservation equation is

$$\frac{1}{r}\frac{\partial}{\partial r}(r\rho v_r h)+\frac{\partial}{\partial z}(\rho v_z h)=\frac{1}{r}\frac{\partial}{\partial r}\left(\frac{r\kappa}{c_p}\frac{\partial h}{\partial r}\right)+\frac{\partial}{\partial z}\left(\frac{\kappa}{c_p}\frac{\partial h}{\partial z}\right)+j_r E_r+j_z E_z-R \tag{4}$$

Current continuity equation is

$$\frac{1}{r}\frac{\partial}{\partial r}(rj_r)+\frac{\partial}{\partial z}(j_z)=0 \tag{5}$$

Ohm's law is

$$j_r=-\sigma E_r, j_z=-\sigma E_z \tag{6}$$

In the above equations, t is the time, h is the enthalpy, P is the pressure, v_z and v_r are the axial and radial velocities, j_z and j_r are the axial and radial component of current density, g is the acceleration owing to gravity, κ is the thermal conductivity, C_p is the specific heat, ρ is the density, η is the viscosity, σ is the electrical conductivity, R is the radiation emission coefficient and E_r and E_z are the radial and axial components of the

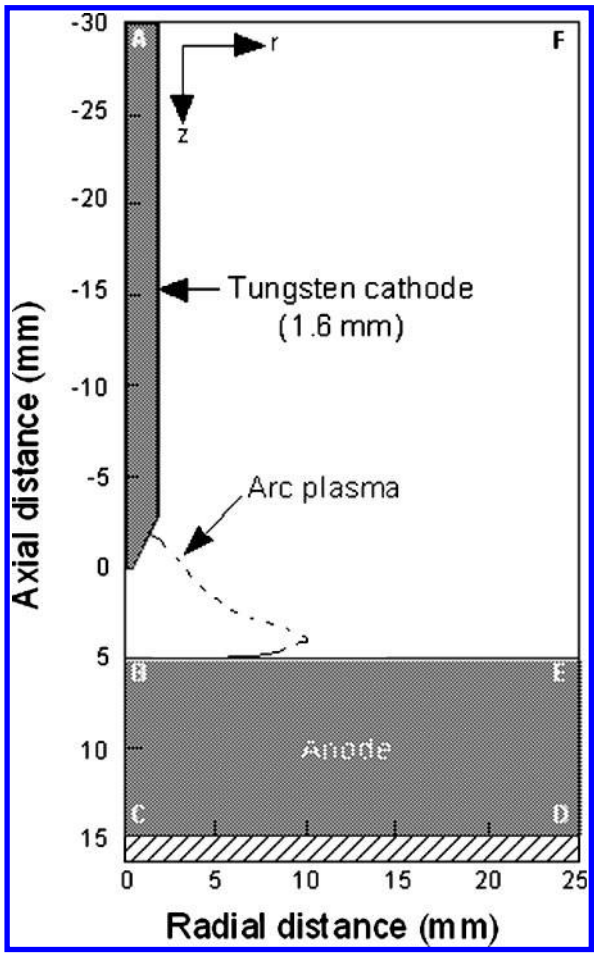

2 Schematic illustration of numerical simulation region

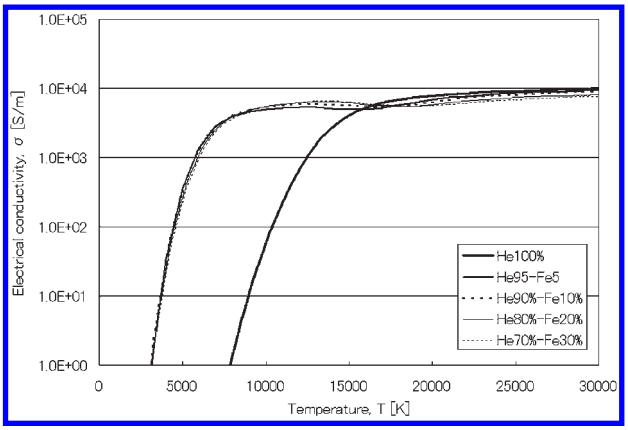

3 Temperature dependence of electrical conductivity for each mixture ratio

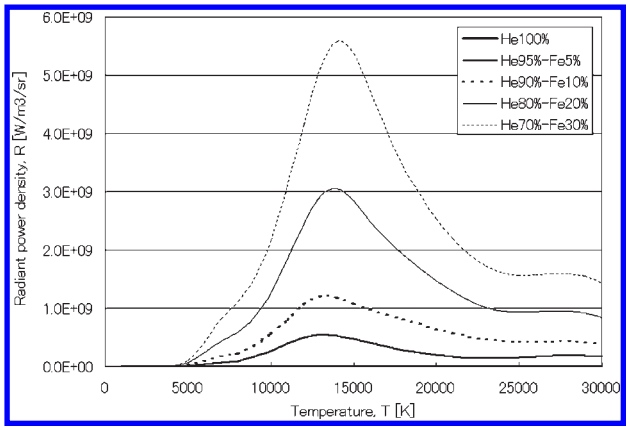

4 Temperature dependence of radiant power density for each mixture ratio

electric field defined by $E_r=-\partial V/\partial r$ and $E_z=-\partial V/\partial z$, where V is the electric potential. The azimuthal magnetic field B_θ induced by the arc current is evaluated by the following Maxwell's equation

$$\frac{1}{r}\frac{\partial}{\partial r}(rB_\theta)=\mu_0 j_z \tag{7}$$

where μ_0 is the permeability in vacuum.

In order to solve the above equations (1)–(6), the special condition about thermal flux that occurs only at the electrode surface must be considered. An additional energy flux term at the cathode surface is needed in equation (4) considering the thermionic cooling owing to the emission of electrons, ion heating and radiation cooling. The additional energy flux for the cathode H_k is defined as

$$H_K=-\varepsilon\alpha T^4-|j_e|\phi_K+|j_i|V_i \tag{8}$$

where ε is the surface emissivity, α is the Stefan–Boltzmann constant, ϕ_K is the work function of the tungsten cathode, V_i is the ionisation potential of argon, j_e is the electron current density and j_i is the ion current density.

As to thermionic emission of electrons at the cathode surface, j_e cannot exceed the Richardson current density J_R[19] given by

$$|j_R|=AT^2\exp\left(-\frac{e\phi_e}{k_B T}\right) \tag{9}$$

where A is the thermionic emission constant for the cathode surface, ϕ_e is the effective work function for thermionic emission of the electrode surface at the local surface temperature and k_B is the Boltzmann's constant. The ion current density j_i is then assumed to be $|j|-|j_R|$ if $|j|$ is greater than $|j_R|$, where $|j|=|j_e|+|j_i|$ is the total current density at the cathode surface obtained from equation (5).

Similarly, for the anode surface, equation (4) needs an additional energy flux term for heating by electron condensation (thermionic heating) and radiation cooling. The additional energy flux for the anode H_A is defined as

$$H_A=-\varepsilon\alpha T^4+|j|\phi_A \tag{10}$$

where ϕ_A is the work function of the anode and $|j|$ is the current density at the anode surface obtained from equation (5). The term ϕ_A accounts for heating of the anode by electrons, which delivers energy equal to that the work function absorbed at the anode. This term is analogous to the cooling effect that occurs at the cathode when electrons are emitted.

The thermodynamic coefficients and transport coefficients are calculated based on the first Chapman–Enskog approximation.[20] The radiation emission coefficients are given in the same manner as reported in the literature.[21] Metal vapour is characterised by its high electrical conductivity and high radiation emission coefficient. The temperature dependence of electrical conductivity and radiation emission coefficients, which is important for the analysis, is presented in Figs. 3 and 4 respectively.

Simulation results and discussion

The simulation results of the distribution of temperature and fluid flow velocity of arc plasma are shown for pure He in Fig. 5, for He–5%Fe in Fig. 6 and for He–30%Fe in Fig. 7. It can be seen that the arc column tends to contract as the iron vapour mixture ratio increases and

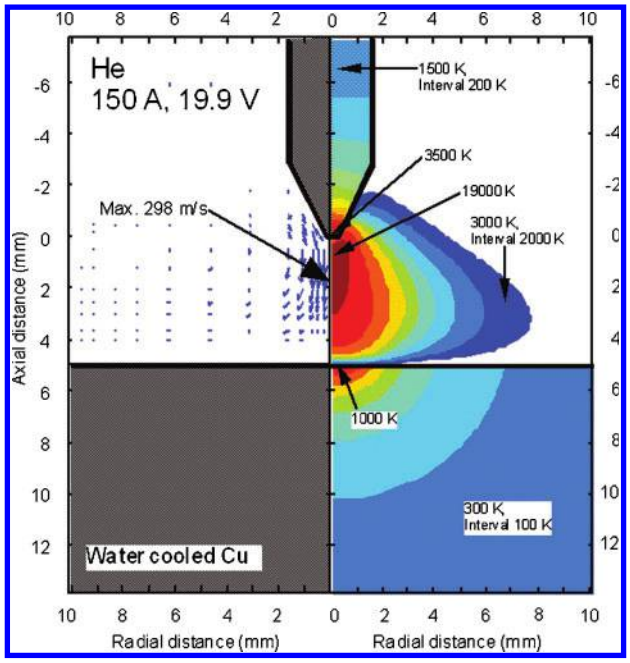

5 Two-dimensional distribution of temperature and fluid flow velocity of arc plasma for pure He

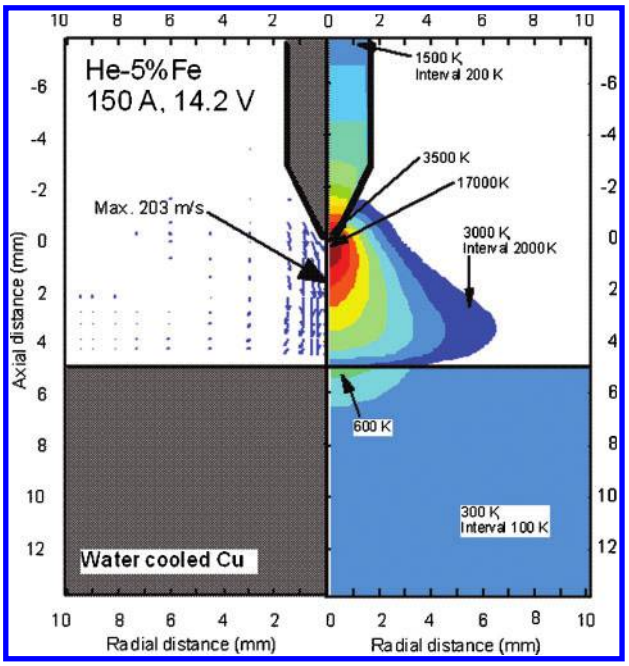

6 Two-dimensional distribution of temperature and fluid flow velocity of arc plasma for He–5%Fe

that the plasma temperature drastically decreases except in the vicinity of the cathode. In fact, the plasma temperature is decreased by 6000 K on the fringe of the arc column (r=2·0 mm) and in the vicinity of the anode (z=4·0 mm), when the mixture ratio of iron vapour is increased from 0 (pure He) to 5%. This simulation result is in well accordance with the experimental one.[4] On the other hand, in the vicinity of the cathode, both the maximum plasma temperature and the maximum cathode jet velocity are reduced below the levels in the case of pure He owing to the mixture of iron vapour of 5%. However, they increase above the levels in the case of pure He when the mixture ratio is raised to 30%.

The general characteristics of metal vapour enhance the electrical conductivity of arc plasma and the

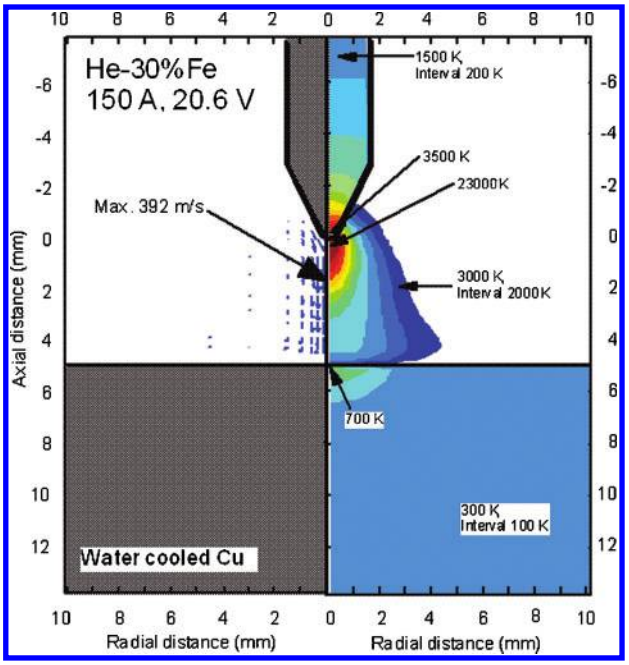

7 Two-dimensional distribution of temperature and fluid flow velocity of arc plasma for He–30%Fe

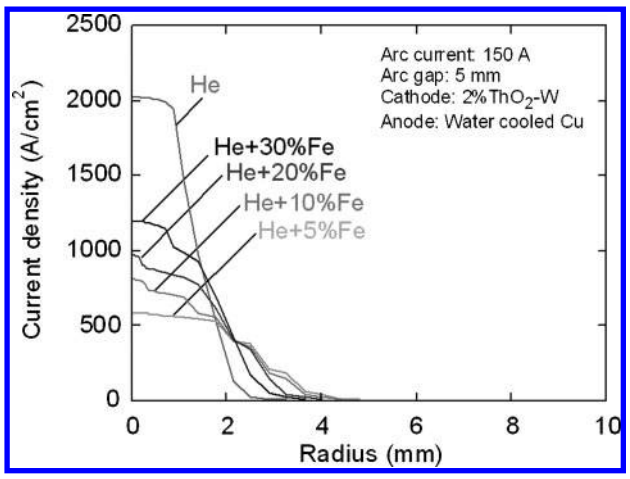

8 Radial distributions of current density at anode surface

radiation heat loss. In fact, only a small amount of metal vapour greatly enhances the electrical conductivity, because the ionisation potential of iron vapour (7·9 eV) is only a third of that of He (24·6 eV). As shown in Fig. 3, this tendency becomes more significant in the lower temperature regions. The electrical conductivity of arc plasma mixed with metal vapour is ten times higher than that of pure He at temperatures <15 000 K. Above this temperature, however, the electrical conductivity does not differ between with and without metal vapour. As to the radiation heat loss, it increases in nearly proportion to the mixture ratio because the radiation by He is negligible.

The results of the radial distribution of current density at the anode surface is shown in Fig. 8. It is found that at relatively lower plasma temperature regions except in the vicinity of the cathode, the mixture of iron vapour of 5% enhances electrical conductivity within the wide radial directions and makes the current density distribution level off. As a result, the plasma temperature in this region decreases owing to the radiation heat loss as well as a decrease in Joule heat.

At the mixture ratio of 10% or higher, the current density distribution tends to contract in the vicinity of the arc axis. Because an increase in electrical conductivity owing to the mixture of iron vapour is saturated at the mixture ratio >5% as shown in Fig. 3, the effect of the radiation heat loss becomes dominant. On the fringe of the arc column, electrical conductivity decreases owing to a decrease in plasma temperature caused by the radiation heat loss. It follows that the current path is restricted in the vicinity of the arc axis and the current density distribution contracts owing to a so called thermal pinch effect.

For the same reason, at the higher plasma temperature region near the cathode, an increase in electrical conductivity owing to the mixture of iron vapour is negligibly small and thus the effect of radiation heat loss on the contraction of the current density distribution becomes dominant. It is considered that at higher mixture ratio the increase in current density caused by the contraction enhances Joule heat and the plasma temperatures and that the electromagnetic pinching force is strengthened at the same time so that cathode jet is accelerated.

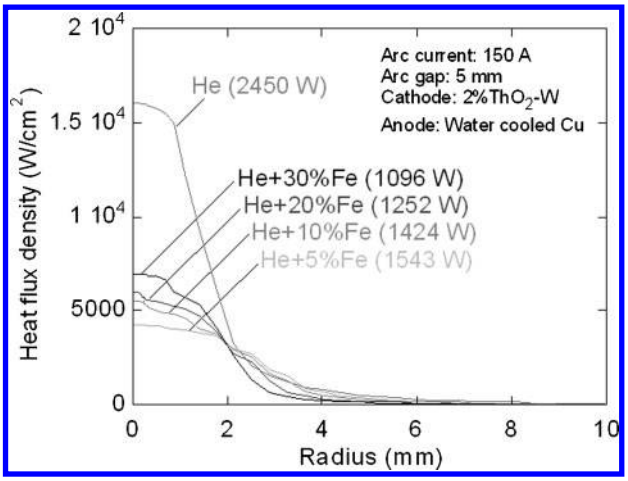

9 Radial distributions of heat flux density at anode surface

The result of the radial distribution of heat flux density to the anode surface is shown in Fig. 9. The result of the iron vapour mixture dependence of the maximum anode surface temperature and the maximum heat flux density to the anode is shown in Fig. 10. The heat flux density consists of that by thermal conduction (Conduction) and that by electron condensation (Electron) which was calculated by equation (10). The decrease in the plasma temperature in the vicinity of the anode reduces the thermal conduction to the anode surface and the electron condensation decreases in proportion to a decrease in the current density. As shown in Fig. 9, at the mixture ratio of 5%, the maximum heat flux density drops to a 30% level of pure He. At the same time the temperature at the anode surface drastically decreases as shown in Fig. 10. At the mixture ratios >5%, the effect of radiation heat loss becomes dominant and the current density distributions contract owing to the same mechanism as a thermal pinch effect so that the heat flux density by electron condensation increases. As a result, the maximum heat flux density and the maximum anode surface temperature slightly increase as the mixture ratio increases >5%.

The calculated result of the iron vapour mixture dependence of input power, heat input to the anode and radiation heat loss is plotted against the left vertical axis

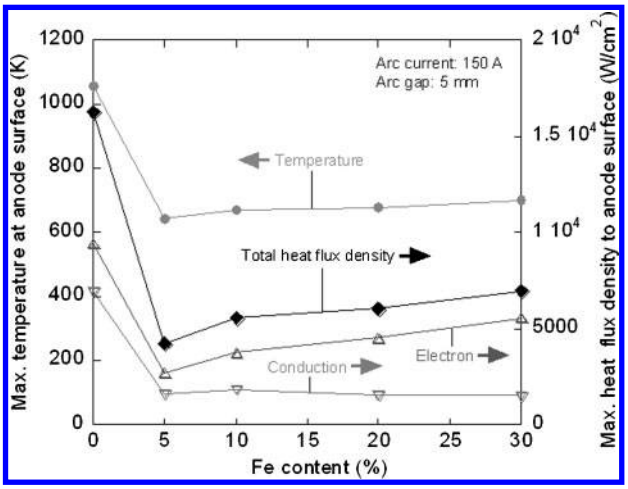

10 Dependence of maximum temperature and heat flux density at anode surface on iron vapour content

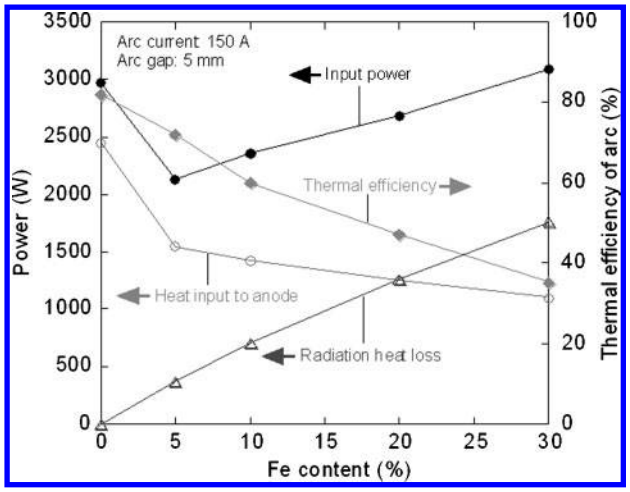

11 Dependence of input power, thermal efficiency, heat input to anode and radiation heat loss on iron vapour content

and that of thermal efficiency of arc is plotted against the right vertical axis in Fig. 11. As shown in Fig. 11, the radiation heat loss increases in nearly proportion to the iron vapour mixture ratio. With an increase in this ratio, the plasma temperature in the vicinity of the anode and thermal conduction to the anode both decrease. It follows that the heat input to the anode decreases in inverse proportion to the mixture ratio. At the mixture ratio <5%, the input power tends to decrease owing to the increase in electrical conductivity but it increases at the mixture ratio >5% in order to compensate the radiation heat loss. As a result, the thermal efficiency drastically decreases with an increase in the mixture ratio, reaching a level <50% at the mixture ratio of 30%.

Conclusions

A numerical analysis was conducted to investigate the arc plasma characteristics of He GTA with the mixture of iron vapour. The characteristics of the heat flux to the water cooled copper anode were also analysed. It was found that the effect of the mixture of metal vapour has to be taken into account in analysing GMA phenomena. The important findings are as follows.

1. Electrical conductivity increases and radiation heat loss is enhanced as the mixture ratio of iron vapour is increased. At the mixture ratio of 5%, the plasma temperature on the fringe of arc column and in the vicinity of the anode is reduced by 6000 K compared with that in the case of pure He.

2. Radiation heat loss of arc plasma contracts arc column as well as the current density distribution, resulting in an increase in the maximum temperature of arc plasma.

3. At the iron vapour mixture ratio of 5%, the maximum heat flux density to the anode lowers to a 30% level of that at 0% ratio (pure He) and the maximum temperature at the anode surface drastically decreases. At the mixture ratios >5%, both the maximum heat flux density and the anode surface temperature tend to increase.

4. At the mixture ratio <5%, input power decreases owing to the effect of an increase in electrical conductivity. However, at the mixture ratio >5%, input power increases in order to compensate the radiation

heat loss. As a result, thermal efficiency significantly decreases with increasing mixture ratio, reaching $<50\%$ at the mixture ratio of 30%.

References

1. K. Etemadi and E. Pfender: *Plasma Chem. Plasma Proc.*, 1985, **5**, 175–182.
2. M. Razafinimanana, L. EI. Hamidi, A. Gleizes and S. Vacquie: *Plasma Sources Sci. Technol.*, 1995, **4**, 501–510.
3. A. M. Rahal, B. Rahhaoui and S. Vacquie: *J. Phys. D*, 1984, **17D**, 1807–1822.
4. H. Terasaki, M. Tanaka and M. Ushio: *Metall. Mater. Trans. A*, 2002, **33A**, 1183–1188.
5. H. Terasaki, M. Tanaka and M. Ushio: *J. Weld. Soc.*, 2002, **20**, 201–206.
6. H. Terasaki: 'Study on physical phenomena of arc plasma Pn GTA Welding', Master thesis, Osaka University, Osaka, Japan, 2000.
7. A. J. D. Farmer, G. N. Haddad and L. E. Cram: *J. Phys. D*, 1986, **19D**, 1723–1730.
8. J. Menart and L. Lin: *Plasma Chem. Plasma Process*, 1999, **19**, 153–170.
9. J. J. Gonzalez, A. Gleizes, P. Proulx and M. Boulos: *J. Appl. Phys.*, 1993, **74**, 3065–3070.
10. H. G. Fan and R. Kovacevic: *J. Phys. D*, 2004, **37D**, 2531–2544.
11. Y. Hirata, K. Ohnishi and T. Ohji: *Preprints Natl Meet. JWS*, 2004, **22**, 80–81. (in Japanese)
12. T. P. Quinn, M. Szanto, I. Gilad and I. Shai: *Sci. Technol. Weld. Join.*, 2005, **10**, 113–119.
13. T. Yamamoto, T. Ohji, F. Miyasaka and Y. Tsuji: *Sci. Technol. Weld. Join.*, 2002, **7**, 260–264.
14. M. Ushio, M. Tanaka and J. J. Lowke: *IEEE Trans. Plasma Sci.*, 2004, **32**, 108–117.
15. M. Tanaka, H. Teresaki, M. Ushio and J. J. Lowke: *Metal. Trans. A*, 2002, **33A**, 2043–2052.
16. M. Tanaka, H. Teresaki, M. Ushio and J. J. Lowke: *Plasma Chem. Plasma Process*, 2003, **23**, 585–606.
17. J. J. Lowke, R. Morrow and J. Haidat: *J. Phys. D*, 1997, **30D**, 1–10.
18. S. V. Patanker: 'Numerical heat transfer and fluid flow'; 1980, Washington, Hemisphere Publishing Corporation.
19. E. Pfender: 'Electric arcs and arc gas heaters', (ed. M. H. Hirsh and H. J. Oskam), Vol. 1, 291–398; 1978, New York, Gaseous Electronics, Academic Press.
20. J. M. Yos: 'Transport properties of nitrogen, hydrogen oxygen, and air to 30000 K', RAD-TM- 63-7, Research and Advanced Development Division AVCO Corporation, Wilmington, MA, 1963.
21. S. Honda, Y. Inoue, T. Iwao, M. Yumoto and T. Inaba: Proc. Tech. Meet. on 'Frontier technology and engineering', 2005, IEE Japan, Paper FTE-05-2.